East Asian Math. J.
Vol. 39 (2023), No. 1, pp. 075–085
http://dx.doi.org/10.7858/eamj.2023.009

NON-OVERLAPPING RECTANGULAR DOMAIN DECOMPOSITION METHOD FOR TWO-DIMENSIONAL TELEGRAPH EQUATIONS

Younbae Jun

Abstract. In this paper, a non-overlapping rectangular domain decomposition method is presented in order to numerically solve two-dimensional telegraph equations. The method is unconditionally stable and efficient. Spectral radius of the iteration matrix and convergence rate of the method are provided theoretically and confirmed numerically by MATLAB. Numerical experiments of examples are compared with several methods.

1. Introduction

The two-dimensional telegraph equation considered on our study is of the form

$$u_{tt} + 2\alpha u_t + \beta^2 u = u_{xx} + u_{yy} + f(x,y,t), (x,y,t) \in \Omega \times [0,T] \tag{1}$$

defined in $\Omega = [0,1] \times [0,1]$, with the initial and boundary conditions

$$u(x,y,0) = u_0(x,y), u_t(x,y,0) = u_1(x,y) \text{ in } \Omega, \tag{2}$$

$$u(x,y,t) = u_b(x,y,t) \text{ on } \partial\Omega, 0 \le t \le T, \tag{3}$$

where T, α and β are given constants.

The equation of the form (1) is commonly applied to describe wave phenomena and the propagation of electrical signals. It also has important applications in other fields, such as chemical and biological fields, electricity, fluid mechanics, elasticity, acoustics, microwave technology, and so on. A growing attention has been paid to the studies of telegraph equation by using various kinds of numerical methods. In [2], a Haar wavelet collocation approach is used for solving one and two-dimensional second-order linear and nonlinear hyperbolic telegraph equations. An application of the singular boundary method is studied in [3] to the two-dimensional telegraph equation on arbitrary domains. Haghighi *et al.* [5] proposed the Fragile Points Method to solve the two-dimensional hyperbolic

Received December 30, 2022; Accepted January 27, 2023.
2010 *Mathematics Subject Classification.* 65M06.
Key words and phrases. Domain decomposition, Finite difference method, Stability, Efficiency, Spectral radius.
This research was supported by Kumoh National Institute of Technology(2020-0197-0001).

(pISSN 1226-6973, eISSN 2287-2833)

telegraph equation using point stiffness matrices. Hesameddini and Asadolahifard [6] considered a new spectral Galerkin method. Lin *et al.* [8] presented an accurate meshless collocation technique. Modified B-spline differential quadrature method is numerically studied in [10]. Mohanty [11] presented an operator splitting method. Zhao *et al.* [13] analyzed a continuous Galerkin method with mesh modification for the two-dimensional telegraph equation.

In recent years, domain decomposition (DD) architecture is often used for solving hyperbolic partial differential equation(PDE), because it very efficient not only on a parallel computer but also on a single process machine. The basic idea of a DD method is that the spatial domain is decomposed into several subdomains and the PDE on each subdomain is solved independently. In [7], an efficient stripwise DD method is analyzed. In this paper, we propose a non-overlapping rectangular DD method to solve two-dimensional telegraph equations. In Section 2, we present the rectangular DD algorithm and discuss its stability with numerical experiments. In Section 3, we analyze the efficiency of the rectangular DD method. Spectral radius of iteration matrix is formulated theoretically and confirmed numerically. Lastly, we make concluding remarks in Section 4.

2. Rectangular DD algorithm and Stability

In this section, we describe our rectangular DD algorithm to solve the initial-boundary value problem(IBVP) (1)–(3) and analyze its stability. Finite difference scheme is used to discretize the PDE and the domain of the problem. We choose positive integers L, M, and N, where $\Delta x = \frac{1}{L}$, $\Delta y = \frac{1}{M}$, and $\Delta t = \frac{T}{N}$. Let $x_i = i\Delta x$, $y_j = j\Delta y$, and $t_n = n\Delta t$, where $i = 0, \cdots, L, j = 0, \cdots, M$, and $n = 0, \cdots, N$. Let u_{ij}^n be the exact solution $u(x_i, y_j, t_n)$ and w_{ij}^n be the approximation of u_{ij}^n. Let f_{ij}^n be $f(x_i, y_j, t_n)$. Then, the central difference operators for each derivative at (x_i, y_j, t_n) are the following:

$$w_{tt}^n = \frac{w_{i,j}^{n+1} - 2w_{ij}^n + w_{i,j}^{n-1}}{(\Delta t)^2}, w_t^n = \frac{w_{ij}^{n+1} - w_{ij}^{n-1}}{2\Delta t},$$

$$w_{xx}^n = \frac{w_{i+1,j}^n - 2w_{ij}^n + w_{i-1,j}^n}{(\Delta x)^2}, w_{yy}^n = \frac{w_{i,j+1}^n - 2w_{ij}^n + w_{i,j-1}^n}{(\Delta y)^2}.$$

2.1. General three-level schemes

There are general finite difference three-level schemes [1, 7] for the problem (1)–(3), which are the fully explicit scheme and fully implicit scheme. We note that these schemes are not domain decomposition methods. However, they are used in this paper to be compared with new method. Stencils of those general three-level schemes are provided in Figure 1.

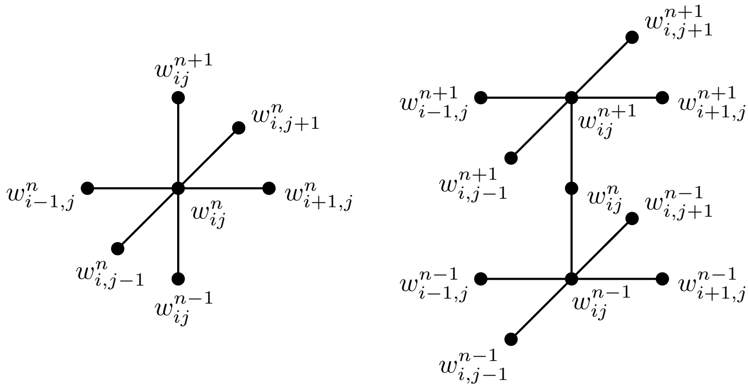

(a) Fully Explicit Scheme (b) Fully Implicit Scheme

Figure 1. Stencils of general three-level schemes

Let us remark on well-known properties [1, 7] of general three-level schemes for the stability to solve the problem (1)–(3).

Remark 2.1. The following fully explicit scheme(FES) is conditionally stable for $\lambda = \left(\frac{\Delta t}{\Delta x}\right)^2 + \left(\frac{\Delta t}{\Delta y}\right)^2 \leq 1$:

$$w_{tt}^n + 2\alpha w_t^n + \beta^2 w_{ij}^n = w_{xx}^n + w_{yy}^n + f_{ij}^n. \tag{4}$$

Remark 2.2. The following fully implicit scheme(FIS) is unconditionally stable:

$$w_{tt}^n + 2\alpha w_t^n + \beta^2 w_{ij}^n = \frac{1}{2}\left(w_{xx}^{n+1} + w_{xx}^{n-1}\right) + \frac{1}{2}\left(w_{yy}^{n+1} + w_{yy}^{n-1}\right) + f_{ij}^n. \tag{5}$$

2.2. Rectangular domain decomposition scheme

We now present our rectangular DD scheme for two-dimensional telegraph equations. Spatial domain may be decomposed into smaller subdomains in the stripwise or rectangular manner. In this paper, we focus on non-overlapping rectangular decomposition. Figure 2 shows a 3×3 rectangular domain decomposition where two adjacent subdomains share an interface line.

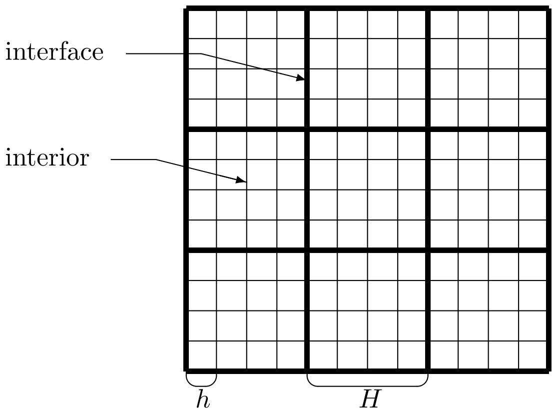

Figure 2. Non-overlapping rectangular decomposition

2.2.1. *Interface prediction.* In order to solve the IBVP (1)–(3) on each subdomain independently, the values of the points at the interface line need to be estimated in advance. Suppose the whole domain is decomposed into $P \times P$ rectangular subdomains and let $H = 1/P$. Define the central finite difference operators $\hat{w}_{xx}^n$ and $\hat{w}_{yy}^n$ on the vertical and horizontal interface lines, respectively, by

$$\hat{w}_{xx}^n = \frac{w_{i+LH,j}^n - 2w_{ij}^n + w_{i-LH,j}^n}{H^2} \text{ and } \hat{w}_{yy}^n = \frac{w_{i,j+MH}^n - 2w_{ij}^n + w_{i,j-MH}^n}{H^2},$$

where $w_{i+LH,j}^n$, $w_{i-LH,j}^n$, $w_{i,j+MH}^n$, and $w_{i,j-MH}^n$ are the unknown values on the interface lines. Then we define the implicit vertical and horizontal interface prediction schemes by

$$w_{tt}^n + 2\alpha w_t^n + \beta^2 w_{ij}^n = \frac{1}{2}\left(\hat{w}_{xx}^{n+1} + \hat{w}_{xx}^{n-1}\right) + \frac{1}{2}\left(w_{yy}^{n+1} + w_{yy}^{n-1}\right) + f_{ij}^n, \quad (6)$$

and

$$w_{tt}^n + 2\alpha w_t^n + \beta^2 w_{ij}^n = \frac{1}{2}\left(w_{xx}^{n+1} + w_{xx}^{n-1}\right) + \frac{1}{2}\left(\hat{w}_{yy}^{n+1} + \hat{w}_{yy}^{n-1}\right) + f_{ij}^n. \quad (7)$$

Stencils of these prediction schemes are provided in Figure 3.

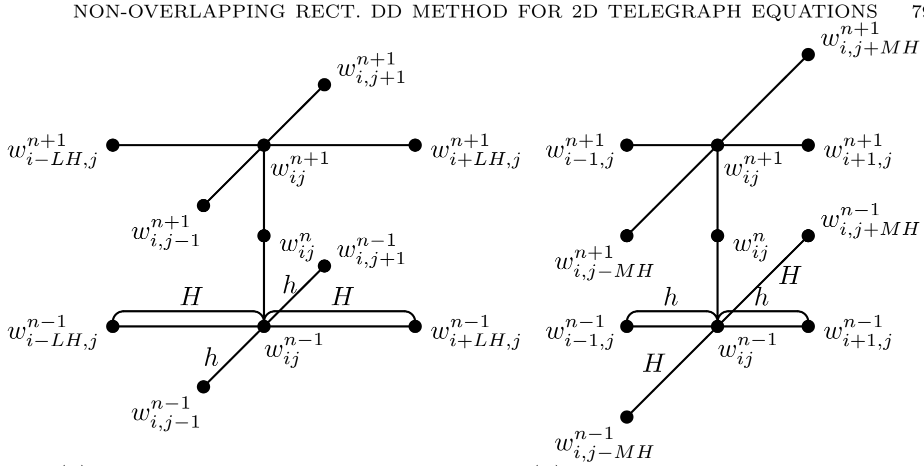

(a) Vertical interface prediction (b) Horizontal interface prediction

Figure 3. Stencils of vertical and horizontal interface prediction

2.2.2. *Interior region.* After estimating interface values, each sub-problem is solved by the fully implicit scheme:

$$w_{tt}^n + 2\alpha w_t^n + \beta^2 w_{ij}^n = \frac{1}{2}\left(w_{xx}^{n+1} + w_{xx}^{n-1}\right) + \frac{1}{2}\left(w_{yy}^{n+1} + w_{yy}^{n-1}\right) + f_{ij}^n.$$

We note that the formula in this step is the same as the FIS, but the number of unknowns of corresponding linear systems are different. Since the whole domain is divided into the smaller subdomains, the number of unknowns over the subdomain interior region is much smaller than the number in the FIS.

Then, we repeat the prediction process and interior region step until the last time level. This whole process is the rectangular domain decomposition algorithm referred to as the RectDD method. We summarize the RectDD algorithm in the following.

Algorithm 2.3. (RectDD algorithm)

Step 1: Predict interface values at the vertical line $x = x_i$ using Eq. (6)

$$w_{tt}^n + 2\alpha w_t^n + \beta^2 w_{ij}^n = \frac{1}{2}\left(\hat{w}_{xx}^{n+1} + \hat{w}_{xx}^{n-1}\right) + \frac{1}{2}\left(w_{yy}^{n+1} + w_{yy}^{n-1}\right) + f_{ij}^n.$$

Step 2: Predict interface values at the horizontal line $y = y_j$ using Eq. (7)

$$w_{tt}^n + 2\alpha w_t^n + \beta^2 w_{ij}^n = \frac{1}{2}\left(w_{xx}^{n+1} + w_{xx}^{n-1}\right) + \frac{1}{2}\left(\hat{w}_{yy}^{n+1} + \hat{w}_{yy}^{n-1}\right) + f_{ij}^n.$$

Step 3: Solve interior linear systems using Eq. (5)

$$w_{tt}^n + 2\alpha w_t^n + \beta^2 w_{ij}^n = \frac{1}{2}\left(w_{xx}^{n+1} + w_{xx}^{n-1}\right) + \frac{1}{2}\left(w_{yy}^{n+1} + w_{yy}^{n-1}\right) + f_{ij}^n.$$

Step 4: Repeat Step 1 through Step 3 until the last time level

Theorem 2.4. *(Stability) Suppose the spatial domain is decomposed into $P \times P$ rectangular subdomains. Then the RectDD method is unconditionally stable and the order of accuracy of the scheme is second.*

Proof. The scheme at the interface is obtained by central differences over the coarse mesh defined by the partition into subdomains, and therefore all of the vertical and horizontal interface prediction schemes and the interior scheme are unconditionally stable. Since $w_{tt}^n = u_{tt} + O((\Delta t)^2)$, $w_t^n = u_t + O((\Delta t)^2)$, $w_{xx}^n = u_{xx} + O((\Delta x)^2)$, $w_{yy}^n = u_{yy} + O((\Delta y)^2)$, $\hat{w}_{xx}^n = u_{xx} + O(H^2)$, and $\hat{w}_{yy}^n = u_{yy} + O(H^2)$, we can clearly observe that the vertical and horizontal interface prediction schemes and the interior scheme of the RectDD method have the errors $|w_{ij}^n - u_{ij}^n| = O(H^2 + (\Delta y)^2 + (\Delta t)^2)$, $|w_{ij}^n - u_{ij}^n| = O((\Delta x)^2 + H^2 + (\Delta t)^2)$ and $|w_{ij}^n - u_{ij}^n| = O((\Delta x)^2 + (\Delta y)^2 + (\Delta t)^2)$, respectively. Thus, the overall RectDD method is unconditionally stable with the second-order accuracy. □

Example 2.5. Let us consider the following two model problems MP1 and MP2 used in [7, 11]:

MP1: $u_{tt} = u_{xx} + u_{yy}$,
MP2: $u_{tt} + 20u_t + 25u = u_{xx} + u_{yy} + 4e^{-t} \sinh x \sinh y$.

Since the RectDD method for these model problems generates very large and sparse linear systems, iterative schemes such as SOR, SSOR, Incomplete Cholesky, or Modified Incomplete Cholesky with acceleration procedure [12] are often used. For simplicity, the Gauss-Seidel (GS) iterative method is used in this paper. The stopping criterion in the iterative procedure is given by

$$\frac{||w^{(n)} - w^{(n-1)}||_2}{||w^{(n)}||_2} < \epsilon,$$

where $w^{(n)}$ is the estimate at the nth GS iteration and $\epsilon = 10^{-6}$ is a preset small value. The numerical experiments in this paper were carried out on a desktop computer with Intel(R) Core(TM) i7-8700 CPU with 8.0GB RAM.

Table 1. Maximum error at the various λ

	$\Delta x (= \Delta y)$	Δt	λ	FES	FIS	RectDD(4×4)
	1/100	1/2	5000	∞	0.5862e-2	0.5793e-2
MP1	1/100	1/5	800	∞	0.1531e-2	0.1743e-2
	1/100	1/10	200	∞	0.1472e-3	0.3330e-3
	1/100	1/50	8	∞	0.8787e-4	0.3368e-4
	1/100	1/2	5000	∞	0.5997e-2	0.5692e-2
MP2	1/100	1/5	800	∞	0.16105e-2	0.16103e-2
	1/100	1/10	200	∞	0.2044e-3	0.2489e-3
	1/100	1/50	8	∞	0.5501e-4	0.1948e-4

Table 1 shows the maximum error $||u^N - w^N||_\infty$ between the exact solution and the approximated solution to the MP1 and MP2 at $t = 1$ with the various

λ from 8 to 5000 of the three methods : FES, FIS, and RectDD with 4×4 subdomains. In Table 1, we see that FES is not convergent for those λ, on the other hand, FIS and RectDD(4×4) are both unconditionally stable. We note that RectDD(4×4) is as accurate as FIS.

3. Efficiency of the Rectangular DD method

In this section, the efficiency of the rectangular DD method is analyzed in terms of the spectral radius of the iteration matrix of the GS iterative method. We first present numerical experiments on the two model problems MP1 and MP2. Table 2 shows the maximum error $||u^N - w^N||_\infty$ and CPU running time at the various decompositions of the RectDD method at the final time level $t = 1$, where $\Delta x = \Delta y = 0.01$, $\Delta t = 0.02$. In Table 2, we see that the various RectDD method are as accurate as the FIS and they are very efficient surprisingly. In addition, the more subdomains of the RectDD we use, the faster convergence we get.

Table 2. Maximum error and CPU time at the various $P \times P$ of the RectDD

	$P \times P$	1(=FIS)	2×2	4×4	10×10	20×20	25×25
	Max. Error	0.878e-4	0.210e-3	0.336e-4	0.245e-4	0.395e-4	0.485e-4
MP1	CPU time	5.46875	5.31250	5.01563	3.89063	2.82813	2.67188
	Max. Error	0.550e-4	0.819e-4	0.194e-4	0.869e-5	0.170e-4	0.223e-4
MP2	CPU time	4.67188	4.54688	4.42188	3.48438	2.57813	2.45313

It is well-known [4, 12] that the rate of convergence of an iterative algorithm is depending on the spectral radius of the iteration matrix. The smaller spectral radius leads to faster convergence in the iterative scheme. Suppose the spatial domain is decomposed into $P \times P$ subdomains. For the sake of simplicity, we consider the RectDD method to the model equation $u_{tt} = u_{xx} + u_{yy}$ and let $h = \Delta x = \Delta y$, $H = 1/P, r = \Delta t/h, \delta = h/H$. Then, the spectral radii of the matrices generated by the GS iteration of each step of the RectDD algorithm are formulated by the following theorems.

Theorem 3.1. *(Rectangular Interior) Suppose the whole domain is decomposed into $P \times P$ subdomains. Let $G_{P\times P}$ be the matrix generated by the Gauss-Seidel iteration of the interior scheme of the RectDD method. Then the spectral radius of $G_{P\times P}$ is*

$$\rho(G_{P\times P}) = \left[\frac{2r^2}{1+2r^2} \cdot \cos P\pi h\right]^2. \tag{8}$$

Proof. Using the five-point finite difference scheme, the coefficient matrix $A_{P\times P}$ of the linear system which arises from the interior scheme can be constructed as

$$A_{P\times P} = \left(1 + \left(\frac{\Delta t}{\Delta x}\right)^2 + \left(\frac{\Delta t}{\Delta y}\right)^2\right) I_K - 4 \cdot \left(\frac{1}{2}r^2\right) R_K = (1+2r^2)I_K - 2r^2 R_K,$$

where I_K is the identity matrix of order K and the matrix R_K is a block tri-diagonal matrix

$$R_K = \frac{1}{4}\begin{bmatrix} S & I & O & \cdots & O \\ I & S & I & \ddots & \vdots \\ O & \ddots & \ddots & \ddots & O \\ \vdots & \ddots & I & S & I \\ O & \cdots & O & I & S \end{bmatrix} \text{ and } S = \begin{bmatrix} 0 & 1 & 0 & \cdots & 0 \\ 1 & 0 & 1 & \ddots & \vdots \\ 0 & \ddots & \ddots & \ddots & 0 \\ \vdots & \ddots & 1 & 0 & 1 \\ 0 & \cdots & 0 & 1 & 0 \end{bmatrix}.$$

The order of the square matrix R_K is $(\frac{L}{P}-1)\cdot(\frac{M}{P}-1)$. It has been proven in [12] that the spectral radius of R_K is

$$\rho(R_K) = \frac{1}{2}\left(\cos\frac{\pi}{L/P} + \cos\frac{\pi}{M/P}\right) = \frac{1}{2}\left(\cos P\pi h + \cos P\pi h\right) = \cos P\pi h.$$

Let the Jacobi iteration matrix $G_{P\times P,J}$ of the interior scheme be

$$G_{P\times P,J} = I_K - \frac{1}{1+2r^2}\{(1+2r^2)I_K - 2r^2R_K\} = \frac{2r^2}{1+2r^2}R_K.$$

Then

$$\rho(G_{P\times P,J}) = \frac{2r^2}{1+2r^2}\rho(R_K) = \frac{2r^2}{1+2r^2}\cdot\cos P\pi h.$$

It is well known [12] that the spectral radius of the GS iteration matrix is equal to the square of the one of the Jacobi iteration matrix. Thus, the spectral radius of the GS iteration matrix of the interior scheme of the Rect-DD method is

$$\rho(G_{P\times P}) = \rho(G_{P\times P,J})^2 = \left[\frac{2r^2}{1+2r^2}\cdot\cos P\pi h\right]^2.$$

□

Theorem 3.2. *(Vertical and horizontal interface predictions) Suppose the whole domain is decomposed into $P\times P$ subdomains and $H = 1/P$. Let $G_{H_{ver}}$ and $G_{H_{hor}}$ be the matrices generated by the Gauss-Seidel iteration of the vertical and horizontal interface prediction schemes of the RectDD method, respectively. Then the corresponding spectral radii are*

$$\rho(G_{H_{ver}}) = \rho(G_{H_{hor}}) = \left[\frac{r^2}{1+\delta^2r^2+r^2}\cdot(\delta^2\cos\pi H + \cos\pi h)\right]^2. \quad (9)$$

Proof. The main diagonal elements of the coefficient matrices $A_{H_{ver}}$ and $A_{H_{hor}}$ for the vertical and horizontal interface schemes are, respectively,

$$1 + \left(\frac{\Delta t}{H}\right)^2 + \left(\frac{\Delta t}{\Delta y}\right)^2 = 1 + \delta^2r^2 + r^2$$

and

$$1 + \left(\frac{\Delta t}{\Delta x}\right)^2 + \left(\frac{\Delta t}{H}\right)^2 = 1 + r^2 + \delta^2r^2.$$

With the same argument as in Theorem 3.1, the coefficient matrices of the linear systems generated by the vertical and horizontal interface prediction schemes can be written as

$$A_{H_{ver}} = (1 + \delta^2 r^2 + r^2) I_{\hat{K}} - 2r^2 R_{\hat{K}},$$

and

$$A_{H_{hor}} = (1 + r^2 + \delta^2 r^2) I_{\hat{K}} - 2r^2 R_{\hat{K}},$$

where

$$R_{\hat{K}} = \frac{1}{4} \begin{bmatrix} \hat{S} & I & O & \cdots & O \\ I & \hat{S} & I & \ddots & \vdots \\ O & \ddots & \ddots & \ddots & O \\ \vdots & \ddots & I & \hat{S} & I \\ O & \cdots & O & I & \hat{S} \end{bmatrix} \text{ and } \hat{S} = \delta^2 \begin{bmatrix} 0 & 1 & 0 & \cdots & 0 \\ 1 & 0 & 1 & \ddots & \vdots \\ 0 & \ddots & \ddots & \ddots & 0 \\ \vdots & \ddots & 1 & 0 & 1 \\ 0 & \cdots & 0 & 1 & 0 \end{bmatrix}.$$

The order $\hat{K}$ of the square matrix $R_{\hat{K}}$ of the interface prediction scheme is $(P-1)\cdot(M-1)$. Following the argument in [12], it can be easily obtained that the spectral radius of $R_{\hat{K}}$ is

$$\rho(R_{\hat{K}}) = \frac{1}{2}\left(\delta^2 \cos\frac{\pi}{P} + \cos\frac{\pi}{M}\right) = \frac{1}{2}\left(\delta^2 \cos\pi H + \cos\pi h\right).$$

The Jacobi iteration matrices $G_{H_{ver},J}$ and $G_{H_{hor},J}$ of the vertical and horizontal interface prediction schemes are the same as

$$I_{\hat{K}} - \frac{1}{1+\delta^2 r^2 + r^2}\{(1+\delta^2 r^2 + r^2) I_{\hat{K}} - 2r^2 R_{\hat{K}}\} = \frac{2r^2}{1+\delta^2 r^2 + r^2} R_{\hat{K}}$$

so that

$$\rho(G_{H_{ver},J}) = \rho(G_{H_{hor},J}) = \frac{2r^2}{1+\delta^2 r^2 + r^2} \cdot \frac{1}{2}(\delta^2 \cos\pi H + \cos\pi h).$$

Thus, the spectral radius of the GS iteration matrix of the vertical and horizontal interface schemes are

$$\rho(G_{H_{ver}}) = \rho(G_{H_{hor}}) = \left[\frac{r^2}{1+\delta^2 r^2 + r^2} \cdot (\delta^2 \cos\pi H + \cos\pi h)\right]^2.$$

□

Corollary 3.3. *Let G_{FIS} be the matrix generated by the GS iteration of the fully implicit scheme. Then the spectral radius of G_{FIS} is*

$$\rho(G_{FIS}) = \left[\frac{2r^2}{1+2r^2} \cdot \cos\pi h\right]^2. \tag{10}$$

Proof. The result is immediately obtained by Theorem 3.1 with $P = 1$. □

Table 3 shows the theoretical spectral radii based on Eq.(8) through Eq.(10) of the GS iteration matrices of the vertical and horizontal interface prediction schemes and the interior region scheme of the RectDD method at the various decompositions for the model problem $u_{tt} = u_{xx} + u_{yy}$ with $\Delta x = \Delta y = 0.01$ and $\Delta t = 0.02$. We see in Table 3 that the spectral radius of the fully implicit scheme is 0.7893. However, the spectral radius of the interior scheme of the RectDD method decreases significantly as $P \times P$ increases. This phenomenon supports the efficiency of the RectDD method, because the smaller spectral radius leads to faster convergence in the iterative method.

Table 3. Theoretical spectral radii at the various $P \times P$ of the RectDD

$P \times P$	1(=FIS)	2×2	4×4	10×10	20×20	25×25
$\rho(G_{H_{ver}})$ Prediction	N/A	**0.6390**	**0.6392**	**0.6413**	**0.6487**	**0.6541**
$\rho(G_{P \times P})$ Interior	**0.7893**	**0.7870**	**0.7777**	**0.7147**	**0.5171**	**0.3951**

Table 4 shows the actual first 6 largest absolute eigenvalues computed by MATALB [9] of the GS iteration matrices of the RectDD method at the various decompositions for the model problem $u_{tt} = u_{xx} + u_{yy}$ with $\Delta x = \Delta y = 0.01$ and $\Delta t = 0.02$. We can see in Table 3 that the largest actual eigenvalue is exactly the same as the theoretical eigenvalue in Table 3.

Table 4. Actual first 6 largest eigenvalues computed by MATLAB

$P \times P$	1(=FIS)	2×2	4×4	10×10	20×20	25×25
		0.6390	**0.6392**	**0.6413**	**0.6487**	**0.6541**
		0.6371	0.6377	0.6395	0.6469	0.6523
Prediction	N/A	0.6339	0.6373	0.6394	0.6469	0.6523
		0.6295	0.6363	0.6376	0.6451	0.6505
		0.6239	0.6358	0.6367	0.6439	0.6493
		0.6171	0.6344	0.6363	0.6438	0.6493
	0.7893	**0.7870**	**0.7777**	**0.7147**	**0.5171**	**0.3951**
	0.7882	0.7824	0.7594	0.6119	0.2469	0.0988
Interior	0.7882	0.7824	0.7594	0.6119	0.2469	0.0988
	0.7870	0.7777	0.7413	0.5171	0.0755	0.0000
	0.7862	0.7746	0.7296	0.4678	0.0494	0.0000
	0.7862	0.7746	0.7296	0.4678	0.0494	0.0000

4. Conclusion

In this paper, we presented a non-overlapping rectangular domain decomposition method for solving two-dimensional telegraph equations. The rectangular DD method was as accurate as the fully implicit scheme and the order of accuracy is second. Furthermore, the rectangular method is much faster than the FIS. Spectral radius of the iteration matrix was formulated theoretically and confirmed numerically. Therefore, the RectDD method is preferable method over the FIS because it is accurate and efficient. Finally, we plan in the future to investigate the relationship between rectangular decomposition and stripwise one.

References

[1] W.F. Ames, Numerical methods for partial differential equations, Academic Press, 1992.

[2] M. Asif, N. Haider, Q. Al-Mdallal, I. Khan, *A Haar wavelet collocation approach for solving one and two-dimensional second-order linear and nonlinear hyperbolic telegraph equations*, Numer. Methods Partial Differential Equations **36** (2020), 1962–1981.

[3] M. Aslefallah, D. Rostamy, *Application of the singular boundary method to the two-dimensional telegraph equation on arbitrary domains*, J. Engrg. Math. **118** (2019), 1–14.

[4] R.L. Burden, J.D. Faires, *Numerical Analysis*, Thomson Brooks/Cole, 2005.

[5] D. Haghighi, S. Abbasbandy, E. Shivanian, L. Dong, S.N. Satya, *The Fragile Points Method (FPM) to solve two-dimensional hyperbolic telegraph equation using point stiffness matrices*, Eng. Anal. Bound. Elem. **134** (2022), 11–21.

[6] E. Hesameddini, E. Asadolahifard, *A new spectral Galerkin method for solving the two dimensional hyperbolic telegraph equation*, Comput. Math. Appl. **72** (2016), 1926–1942.

[7] Y. Jun, *Efficiency analysis of a domain decomposition method for the two-dimensional telegraph equations*. East Asian Math. J. **37** (2021), 295–305.

[8] J. Lin, F. Chen, Y. Zhang, J. Lu, *An accurate meshless collocation technique for solving two-dimensional hyperbolic telegraph equations in arbitrary domains*, Eng. Anal. Bound. Elem. **108** (2019), 372–384.

[9] MATHWORKS, Inc. http://www.mathworks.com.

[10] R.C. Mittal, R. Bhatia, *A numerical study of two dimensional hyperbolic telegraph equation by modified B-spline differential quadrature method*, Appl. Math. Comput. **244** (2014), 976–997.

[11] R.K. Mohanty, *An operator splitting method for an unconditionally stable difference scheme for a linear hyperbolic equation with variable coefficients in two space dimensions*, Appl. Math. Comput. **152** (2004), 799–806.

[12] D.M. Young, *Iterative Solution of Large Linear Systems*, Dover, New York, 2003.

[13] Z. Zhao, H. Li, Y. Liu, *Analysis of a continuous Galerkin method with mesh modification for two-dimensional telegraph equation*, Comput. Math. Appl. **79** (2020), 588–602.

Younbae Jun

Department of Mathematics and Big Data Science, Kumoh National Institute of Technology, Gyeongbuk 39177, Republic of Korea

Email address: `yjun@kumoh.ac.kr`